Current Biology 18, 730–734, May 20, 2008 ©2008 Elsevier Ltd All rights reserved DOI 10.1016/j.cub.2008.04.039

Report

Two MscS Homologs Provide Mechanosensitive Channel Activities in the *Arabidopsis* Root

Elizabeth S. Haswell,[1,3,4,*] Rémi Peyronnet,[2,3] Hélène Barbier-Brygoo,[2] Elliot M. Meyerowitz,[1] and Jean-Marie Frachisse[2]

[1]Division of Biology 156-29
California Institute of Technology
Pasadena, California 91125

[2]Institut des Sciences du Végétal
Centre National de la Recherche Scientifique
UPR 2355
Avenue de la Terrasse
91198 Gif sur Yvette Cedex
France

Summary

In bacterial and animal systems, mechanosensitive (MS) ion channels are thought to mediate the perception of pressure, touch, and sound [1–3]. Although plants respond to a wide variety of mechanical stimuli, and although many mechanosensitive channel activities have been characterized in plant membranes by the patch-clamp method, the molecular nature of mechanoperception in plant systems has remained elusive [4]. Likely candidates are relatives of MscS (Mechanosensitive channel of small conductance), a well-characterized MS channel that serves to protect *E. coli* from osmotic shock [5]. Ten MscS-Like (MSL) proteins are found in the genome of the model flowering plant *Arabidopsis thaliana* [4, 6, 7]. MSL2 and MSL3, along with MSC1, a MscS family member from green algae, are implicated in the control of organelle morphology [8, 9]. Here, we characterize MSL9 and MSL10, two MSL proteins found in the plasma membrane of root cells. We use a combined genetic and electrophysiological approach to show that MSL9 and MSL10, along with three other members of the MSL family, are required for MS channel activities detected in protoplasts derived from root cells. This is the first molecular identification and characterization of MS channels in plant membranes.

Results and Discussion

MSL9 and MSL10 Are Found in the Plasma Membrane of Root Cells

MSL9 and *MSL10* encode proteins of 742 and 734 amino acids, respectively, each with six predicted transmembrane (TM) helices [10]. Unlike MscS, which has its N terminus in the periplasmic space and its C terminus in the cytoplasm [11], MSL9 and MSL10 are predicted to fold with both the N terminus and the C terminus in the cytoplasm, on the basis of charge-bias analysis [10]. As shown in the sequence alignment in Figure 1A, MSL9 and MSL10 are highly similar to each other (75% identical) and to three additional members of the *Arabidopsis* MSL family, MSL4, MSL5, and MSL6 (42% identical) within the highly conserved MscS domain.

To begin to study the function of MSL9 and MSL10, we characterized their expression patterns. GUS reporter-gene expression analysis (Figures 1B–1E) and RT-PCR experiments (Figure S1 in the Supplemental Data available online) show that *MSL9* and *MSL10* are expressed in overlapping but nonidentical patterns. The *MSL9* promoter drives expression in the epidermis, cortex, and endodermis of the root tip (Figures 1B and 1C), and the *MSL10* promoter drives expression in the root tip and throughout the vasculature of the root and leaf (Figures 1D and 1E). These gene expression patterns are in accordance with those reported for *MSL9* (locus identifier 245944) and *MSL10* (locus identifier 250326) in a tissue- and stage-dependent analysis of the *Arabidopsis* root [12].

We used fluorescent protein fusions to analyze the subcellular localization of MSL9 and MSL10 because no signal sequences were apparent in either protein sequence. When expressed under the control of their endogenous promoters, MSL9∼GFP and MSL10∼GFP were observed at the cell periphery, and the strongest signal was at the apical or basal ends of cells in the epidermis of the root tip (Figures 1F and 1H). This apical or basal localization might have functional implications. However, counterstaining the cell wall with propidium iodide revealed that the brightest GFP fluorescence was associated with newly formed cell plates (compare the region marked by arrows in Figures 1F and 1G). Localization to the cell plate has been observed with several root plasma-membrane proteins, including PIN1, PIN2, PIP2, and ARL2 [13, 14], and is thought to be a general by-product of cell-plate formation through endocytosis from the plasma membrane. Furthermore, MSL10∼GFP (Figure 1I) and MSL9∼GFP (data not shown) were found in Hechtian strands; these thin strands of plasma membrane form as the protoplast shrinks away from the cell wall during plasmolysis. Consistent with localization of MSL9 and MSL10 to the plasma membrane, peptides from MSL10 were identified in two independent proteomic analyses of *Arabidopsis* plasma-membrane proteins [15, 16]. In addition, we routinely observed MSL9∼GFP and MSL10∼GFP in internal membranes even when they were expressed from their endogenous promoters. Taken together, these data suggest that MSL9 and MSL10 are primarily localized to the plasma membrane and that a smaller fraction is localized to other internal membranes.

Identification of MS Channels in *Arabidopsis* Root Protoplasts

To determine whether MSL9 or MSL10 provide MS channel activities in the plasma membrane of root cells, we used the patch-clamp technique to analyze protoplasts from wild-type and mutant plants. The main ionic conditions were 150 mM KCl internal and 50 mM $CaCl_2$ external (details are available in the Supplemental Experimental Procedures). We first used the whole-cell configuration because this approach allowed us to survey the main channel activities present in the plasma membrane in the most physiologically relevant patch-clamp configuration. The voltage was clamped at

*Correspondence: ehaswell@wustl.edu
[3]These authors contributed equally to this work.
[4]Present address: Department of Biology, Campus Box 1137, Washington University, One Brookings Road, St. Louis, Missouri 63130.

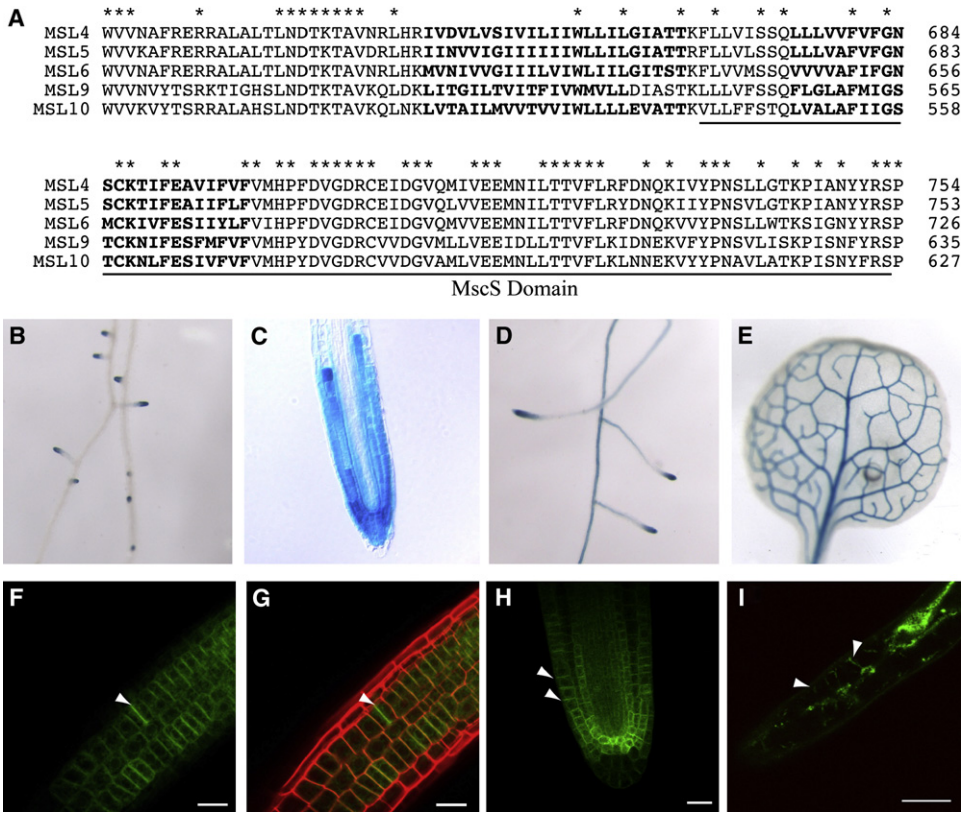

Figure 1. MSL9 and MSL10 Are MscS-Like Proteins Found in the Plasma Membrane of Root Cells

(A) Alignment of the region most highly conserved between MSL9, MSL10, and three other MSL proteins from *Arabidopsis*. Identical residues are marked with asterisks, the predicted transmembrane helices (TM5 and TM6) are indicated in bold type, and the conserved MscS domain is underlined.

(B–E) Representative images of 5- to 10-day-old transgenic plants expressing *MSL9* and *MSL10* GUS reporter genes. (B) MSL9p::GFPGUS lines show activity in the tip of the seedling root. (C) A section from a plastic-embedded root tip from a seedling expressing MSL9p::GFPGUS. A GUS-stained root (D) and leaf (F) from transgenic MSL10p::GFPGUS seedlings.

(F–I). Subcellular localization of MSL9 ~ GFP and MSL10 ~ GFP fusion proteins. The coding sequences of *MSL9* and *MSL10* were fused to the open reading frame of Green Fluorescent Protein (GFP) at the C-termini and expressed under the control of their endogenous promoters in wild-type *Arabidopsis* plants. Multiple lines for each transgene were analyzed by confocal laser scanning microscopy. The primary root tip of a plant expressing MSL9p::MSL9 ~ GFP shows GFP signal (F) and GFP signal overlaid with propidium iodide signal marking the cell wall (G). Arrows indicate newly formed cell plates. (H) Lateral root bud of a plant expressing MSL10p::MSL10 ~ GFP. Arrows indicate strong GFP signal at the apical and basal sides of cells. (I) Root hair from a plant expressing 35Sp::MSL10 ~ GFP, plasmolyzed for 5 min in 5 M NaCl. Arrows indicate GFP signal in Hechtian strands. Scale bars represent 20 μm in (F), (G), and (H) and 10 μm in (I).

−182 mV, which is within the range of the resting membrane potential previously measured in root cells [17–19] and which reduces background activity from the anion channels already characterized in *Arabidopsis* protoplasts [20, 21]. We chose to work with protoplasts derived from root cortical tissue because they were a more homogeneous population than cells from the root tip and because they routinely formed good seals with the patch pipette. Protoplasts derived from the root tip gave the same results as shown below for cortical cells (our unpublished data). As shown in Figure S2A, unitary MS channel-opening events could be resolved in *Arabidopsis* root protoplasts with the whole-cell configuration. To determine the nature of the ions permeating through the WT MS channel, we replaced the external calcium (Figure S3A) or internal chloride (Figure S3B) with the large TEA and MES ions, respectively. Results presented in Figure S3 indicate that under our standard ionic conditions, the wild-type MS channel is more permeant for Cl^- than Ca^{2+}. Using these conditions, we compared the MS activities present in wild-type and mutant plants.

MSL9 and MSL10 Are Required for a Mechanosensitive Activity in the Plasma Membrane of *Arabidopsis* Root Protoplasts

To determine whether *MSL9*, *MSL10*, or both are required for the MS channel observed under these conditions, we analyzed channel activity recordings from plants harboring T-DNA insertions in both *MSL9* and *MSL10* (Figure 2A). *MSL9* transcripts were absent, and *MSL10* transcripts were greatly reduced in root tissue from *msl9-1;msl10-1* double-mutant plants (Figure 2B). Figures 2C–2F present channel activity recordings and amplitude histogram analyses of protoplasts derived from wild-type and mutant plants. These histograms present our measurements of current amplitudes at −182 mV; 2–8 mm Hg positive pressure was used on all protoplasts tested. Only the main peak of each histogram was fitted to unimodal Gaussian curves, and each peak value was determined by the fit curve. The mean recording time analyzed per protoplast was ~60 s, and 32 events were analyzed on average per record. With all wild-type protoplasts tested (n = 38), increasing the pipette pressure induced a channel activity characterized

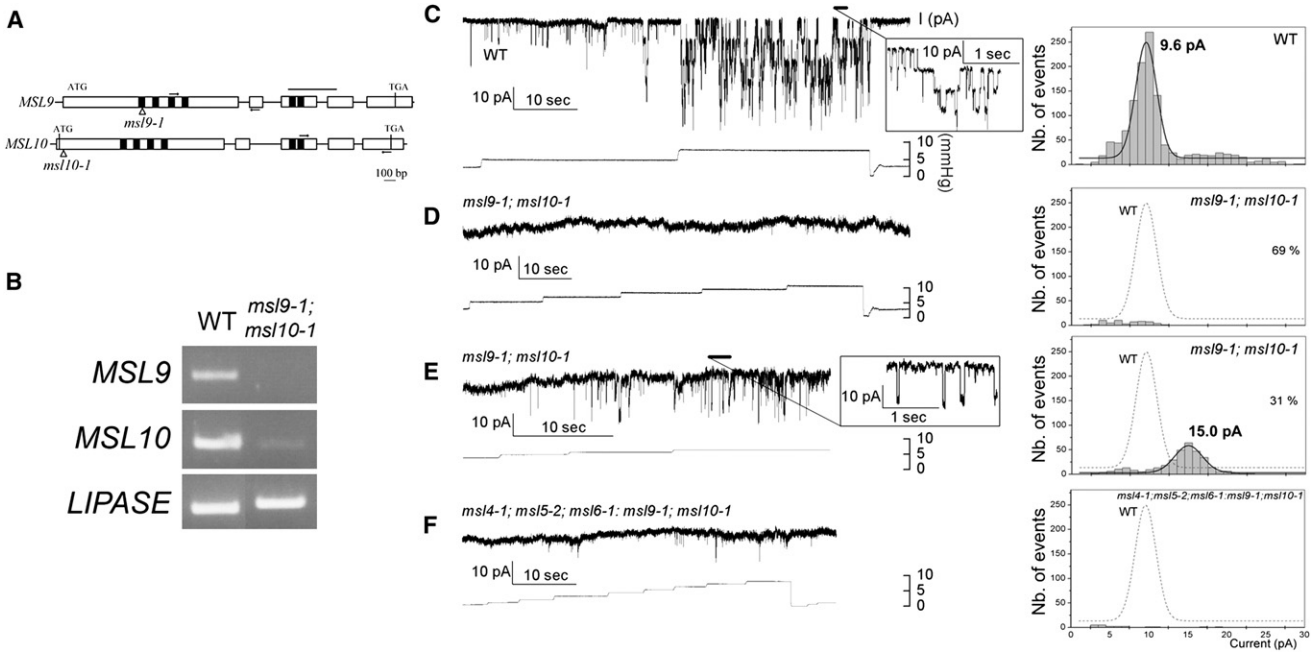

Figure 2. *mscs-like* Mutant Plants Lack the 10 pA Stretch-Activated Channel Activity Characteristic of Wild-Type Plants

(A) Structures of the *MSL*9 and *MSL10* genes and the location of T-DNA inserts. Arrows indicate the approximate location and direction of the primers used for RT-PCR. Black lines indicate the MscS-similar regions that are shown in Figure 1A.

(B) Agarose gel showing semiquantitative RT-PCR products from wild-type and double-mutant root tissue. The *LIP* gene is used as a loading control.

(C–F) Representative traces from whole-cell patch-clamp experiments performed on wild-type and mutant protoplasts, along with a current-amplitude distribution histogram for each genotype. (C) Characteristic 9.6 pA MS channel activity of protoplasts from wild-type plants. (D and E) Either no unitary channel activity or 15.0 pA channel activity was observed in *msl9-1;msl10-1* protoplasts. (F) No unitary channel activity was observed in *msl4-1;msl5-2;msl6-1;msl9-1;msl10-1* plants. Current amplitudes were determined from the difference between the peak and baseline currents during an opening. Amplitude distribution histograms for each trace were fitted to a Gaussian curve, and the mean peak amplitude is indicated. Ionic conditions are described in the Supplemental Experimental Procedures.

by an average amplitude of 9.6 ± 0.1 pA (Figure 2C) and a highly variable open time (682 ± 754 ms, SD). The fact that this wild-type activity was abolished in all *msl9-1;msl10-1* double-mutant protoplasts examined (n = 54) shows that it requires MSL9 and/or MSL10. In a subset of the *msl9-1;msl10-1* mutant protoplasts (69%), no stretch-activated channel activity was detected at any pressure tested (Figure 2D). In the other subset (31%), a distinct stretch-activated channel, with an average amplitude of 15.0 ± 0.1 pA, was detected (Figure 2E).

The activity present in a subset of *msl9-1;msl10-1* mutant protoplasts could be attributed to the action of MSL4, MSL5, or MSL6, three additional members of the MSL family that are also expressed in root cells (Figure S1). To test this, we generated the quintuple mutant *msl4-1;msl5-2;msl6-1;msl9-1;msl10-1* by crossing the *msl9-1;msl10-1* double mutant to a triple *msl4-1;msl5-2;msl6-1* mutant. Semiquantitative RT-PCR analysis of RNA isolated from root tissue showed no detectable transcripts from *MSL4*, *MSL5*, or *MSL6* in the triple mutant (Figure S4). No MS channel activity was detected in any of the *msl4-1;msl5-2;msl6-1;msl9-1;msl10-1* quintuple-mutant protoplasts we examined (n = 33) (Figure 2F). These data show that the MS channel activities detected under our conditions require the MSL family of proteins. The predominant 10 pA activity observed in wild-type protoplasts requires MSL9 and/or MSL10, and the 15 pA channel activity sporadically observed is due to one or more of the MSL4, MSL5, or MSL6 proteins.

MSL9 and MSL10 Have Distinct Stretch-Activated Channel Activities

In order to determine whether MSL9 or MSL10 provides the 10 pA activity characteristic of wild-type plants, *msl9-1* or *msl10-1* single-mutant protoplasts were analyzed. Unexpectedly, the wild-type 10 pA activity was not detected in either of the single mutants; rather, each displayed a different stretch-activated activity characterized by a specific single channel amplitude. In *msl9-1* mutant protoplasts (n = 5), single channel amplitudes with a peak at 19.9 ± 0.2 pA were measured (Figure 3A), and in *msl10-1* mutant protoplasts (n = 15) single channel amplitudes with a peak at 7.3 ± 0.1 pA were measured (Figure 3B). Furthermore, transient expression of *MSL10* in *msl9-1;msl10-1* mutant protoplasts produced activities with a peak at 21.1 ± 0.2 pA (n = 4), and *MSL9* expression produced activities with a peak at 8.0 ± 0.2 pA (n = 5) (Figures 3C and 3D). These data show that in the absence of MSL9, MSL10 forms a channel with an approximately 20 pA current (both when endogenously expressed in the *msl9-1* mutant and when transiently expressed in the *msl9-1;msl10-1* mutant). Similarly, MSL9 forms a channel with an approximately 8 pA current in the absence of MSL10, either when MSL9 is endogenously expressed in the *msl10-1* mutant or when it is transiently expressed in the *msl9-1;msl10-1* mutant.

Each single mutant could be complemented with the missing protein by transient expression. Transient expression of MSL10 in *msl10-1* protoplasts rescued the wild-type activity and produced a channel with an average amplitude of 9.8 ± 0.2 pA

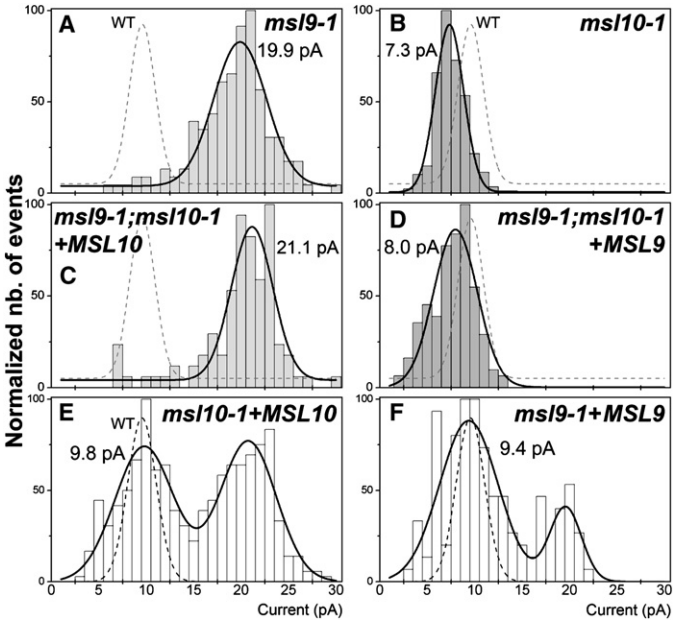

Figure 3. MSL9 and MSL10 Separately Provide Two Different Mechanosensitive Activities, and Complementation of Each Single Mutant Restores the 10 pA Wild-Type Activity

(A and C) Activity of the MSL10-dependent channel. MSL10 activity was detected when the protein was expressed from the endogenous gene in *msl9-1* single mutants (A) or when it was transiently expressed in *msl9-1;msl10-1* mutants (C).

(B and D) Activity of the MSL9-dependent channel. MSL9 activity was detected when the protein was expressed from the endogenous gene in *msl10-1* single mutants (B) or when it was transiently expressed in *msl9-1;msl10-1* mutants (D).

(E) Expression of *MSL10* in *msl10-1* mutant protoplasts rescues the wild-type activity.

(F) Expression of *MSL9* in *msl9-1* mutant protoplasts rescues the wild-type activity. For each genotype the peak of number of events counted (between 99 and 1201) was normalized at 100%. Distributions of events were fitted by unimodal or multimodal Gaussian curves. The curve for the wild-type activity was superimposed as a dashed line for comparison. Ionic conditions were as described in the Supplemental Experimental Procedures.

(n = 7) (Figure 3E). We attribute the additional peak, with an average amplitude of 20.7 pA, to the production of the ~20 pA channel activity that is associated with MSL10 alone; in this case, the activity is produced by transient overexpression of *MSL10*. Transient expression of *MSL9* in *msl9-1* protoplasts (n = 4) also rescued the wild-type activity with an amplitude peak of 9.4 ± 0.2 pA (Figure 3F). In this case, the small peak at 19.5 pA corresponds to the normal activation profile of the *msl9-1* mutant and is associated with the endogenous MSL10-dependent channel. These results strongly suggest that the mechanosensitive channel activity with the ~10 pA current observed in wild-type protoplasts is provided by both MSL9 and MSL10.

To further characterize the wild-type, the MSL9-dependent, and the MSL10-dependent channels, we calculated their conductance (Figure 4). The conductance of the wild-type channel was 54 ± 4 pS in our standard conditions. The conductance of the MSL9-dependent channel, as measured in the *msl10-1* single mutant, was 45 ± 2 pS. The conductance of the MSL10-dependent channel, as measured in the double

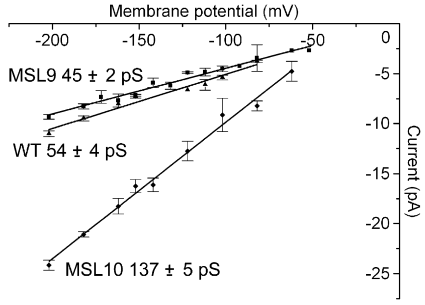

Figure 4. I/V Curves for Wild-Type and MSL9- and MSL10-Dependent Channel Activities

Protoplasts from wild-type plants, *msl10-1* mutants, or *msl9-1;msl10-1* double mutants transiently expressing *MSL10* were patched in the whole-cell configuration. Ionic conditions were as described in the Supplemental Experimental Procedures. Error bars indicate the standard error of the values obtained from n = 8 (wild-type), n = 5 (MSL9), or n = 7 (MSL10) protoplasts at each point in the curve.

msl9-1;msl10-1 mutant transiently expressing *MSL10*, was 137 ± 5 pS. Although these conductance measurements are 10- to 4-fold smaller than those of MscS and MSC1 under similar ionic conditions [8, 22], they are still among the highest described for any ion channel in plant membranes. These results could be explained by a model wherein homomeric complexes of MSL9 and MSL10 have distinct electrophysiological signatures, different from each other and from that of the heteromeric MSL9-MSL10 complex that is present in the wild-type plant. This phenomenon has been documented in several families of ion channels and is thought to provide organisms with an increased diversity of ion-channel activities [23, 24]. Biochemical and electrophysiological studies performed with recombinant proteins will be required for testing the hypothesis that MSL9 and MSL10 form heteromeric complexes.

We used the excised patch conformation to further characterize the activities present in *msl9-1;msl10-1* mutant protoplasts transiently expressing MSL10. A slow pressure ramp was performed, and a channel with an amplitude of about 20 pA at −182 mV was present (Figure S5). In this configuration, we were able to use pressures from 0–90 mm Hg (higher pressures cause membrane rupture), and the activities we observed had the same unitary channel amplitudes as in the whole-cell configuration, and no new channel activities were observed. The activation threshold for this channel was 45–55 mm Hg and did not change significantly from one patch to another. This threshold is slightly lower than that of either MscS (50–100 mm Hg) or MSC1 (130 mm Hg) [8, 25, 26].

Conclusions

The results presented here provide a potential molecular mechanism for mechanosensing in vascular plants. We show that two MscS homologs, MSL9 and MSL10, are expressed in the *Arabidopsis* root, where they are found in the plasma membrane. MSL9 and MSL10 can function independently as MS channels with a conductance of ~45 pS and ~137 pS, respectively, whereas the ~54 pS channel activity characteristic of wild-type root protoplasts requires both MSL9 and MSL10. Alhough we see a clear phenotype at the cellular level in *msl9-1;msl10-1* mutants (the absence of stretch-activated channel

activity), the global physiological role of MSL9 and MSL10 remains unknown. Neither *msl9-1;msl10-1* double mutants nor *msl4-1;msl5-2;msl6-1;msl9-1;msl10-1* quintuple mutants are distinguishable from the wild-type when grown under a variety of osmotic, salt, mechanical, dehydration, or rehydration stresses (details are available in the Supplemental Experimental Procedures). The relatively high conductance reported here suggests that MscS-Like channels may act to rapidly depolarize the membrane or to alter the turgor pressure of plant cells in response to mechanical force. We anticipate that further investigation will reveal how MscS-Like proteins function in multicellular eukaryotes.

Supplemental Data

Experimental Procedures, five figures, and one table are available with this article online at http://www.current-biology.com/cgi/content/full/18/10/730/DC1/.

Acknowledgments

This work was funded by the French Ministry of Research, the Centre National de la Recherche Scientifique, and the U.S. Department of Energy (grant DE-FG02-88ER13873). We thank the Salk Institute Genomic Analysis Laboratory for providing the sequence-indexed *Arabidopsis* T-DNA insertion mutants used in this study.

Received: February 20, 2008
Revised: April 9, 2008
Accepted: April 11, 2008
Published online: May 15, 2008

References

1. Kung, C. (2005). A possible unifying principle for mechanosensation. Nature *436*, 647–654.
2. Vogel, V., and Sheetz, M. (2006). Local force and geometry sensing regulate cell functions. Nat. Rev. Mol. Cell Biol. *7*, 265–275.
3. Hamill, O.P., and Martinac, B. (2001). Molecular basis of mechanotransduction in living cells. Physiol. Rev. *81*, 685–740.
4. Haswell, E.S. (2007). MscS-Like Proteins in Plants. In Mechanosensitive Ion Channels, Part A, *Volume 58*, O.P. Hamill, ed. (San Diego, CA: Academic Press).
5. Levina, N., Totemeyer, S., Stokes, N.R., Louis, P., Jones, M.A., and Booth, I.R. (1999). Protection of Escherichia coli cells against extreme turgor by activation of MscS and MscL mechanosensitive channels: Identification of genes required for MscS activity. EMBO J. *18*, 1730–1737.
6. Pivetti, C.D., Yen, M.R., Miller, S., Busch, W., Tseng, Y.H., Booth, I.R., and Saier, M.H., Jr. (2003). Two families of mechanosensitive channel proteins. Microbiol. Mol. Biol. Rev. *67*, 66–85.
7. Kloda, A., and Martinac, B. (2002). Common evolutionary origins of mechanosensitive ion channels in Archaea, Bacteria and cell-walled Eukarya. Archaea *1*, 35–44.
8. Nakayama, Y., Fujiu, K., Sokabe, M., and Yoshimura, K. (2007). Molecular and electrophysiological characterization of a mechanosensitive channel expressed in the chloroplasts of Chlamydomonas. Proc. Natl. Acad. Sci. USA *104*, 5883–5888.
9. Haswell, E.S., and Meyerowitz, E.M. (2006). MscS-like proteins control plastid size and shape in Arabidopsis thaliana. Curr. Biol. *16*, 1–11.
10. Krogh, A., Larsson, B., von Heijne, G., and Sonnhammer, E.L. (2001). Predicting transmembrane protein topology with a hidden Markov model: Application to complete genomes. J. Mol. Biol. *305*, 567–580.
11. Miller, S., Bartlett, W., Chandrasekaran, S., Simpson, S., Edwards, M., and Booth, I.R. (2003). Domain organization of the MscS mechanosensitive channel of Escherichia coli. EMBO J. *22*, 36–46.
12. Birnbaum, K., Shasha, D.E., Wang, J.Y., Jung, J.W., Lambert, G.M., Galbraith, D.W., and Benfey, P.N. (2003). A gene expression map of the Arabidopsis root. Science *302*, 1956–1960.
13. Dhonukshe, P., Baluska, F., Schlicht, M., Hlavacka, A., Samaj, J., Friml, J., and Gadella, T.W., Jr. (2006). Endocytosis of cell surface material mediates cell plate formation during plant cytokinesis. Dev. Cell *10*, 137–150.
14. Harrison, B.R., and Masson, P.H. (2008). ARL2, ARG1 and PIN3 define a gravity signal transduction pathway in root statocytes. Plant J. *53*, 380–392.
15. Nuhse, T.S., Stensballe, A., Jensen, O.N., and Peck, S.C. (2003). Large-scale analysis of in vivo phosphorylated membrane proteins by immobilized metal ion affinity chromatography and mass spectrometry. Mol. Cell. Proteomics *2*, 1234–1243.
16. Benschop, J.J., Mohammed, S., O'Flaherty, M., Heck, A.J., Slijper, M., and Menke, F.L. (2007). Quantitative phosphoproteomics of early elicitor signaling in Arabidopsis. Mol. Cell. Proteomics *6*, 1198–1214.
17. Maathuis, F.J., and Sanders, D. (1994). Mechanism of high-affinity potassium uptake in roots of Arabidopsis thaliana. Proc. Natl. Acad. Sci. USA *91*, 9272–9276.
18. McClure, P.R., Kochian, L.V., Spanswick, R.M., and Shaff, J.E. (1990). Evidence for cotransport of nitrate and protons in maize roots: II. Measurement of NO(3) and H fluxes with ion-selective microelectrodes. Plant Physiol. *93*, 290–294.
19. Felle, H.H., Kondorosi, E., Kondorosi, A., and Schultze, M. (1995). Nod signal-induced plasma membrane potential chanes in alfalfa root hairs are differentially sensitive to structural modification of the lipochitooligosacchaaride. Plant J. *7*, 939–947.
20. Frachisse, J.M., Colcombet, J., Guern, J., and Barbier-Brygoo, H. (2000). Characterization of a nitrate-permeable channel able to mediate sustained anion efflux in hypocotyl cells from Arabidopsis thaliana. Plant J. *21*, 361–371.
21. Frachisse, J.M., Thomine, S., Colcombet, J., Guern, J., and Barbier-Brygoo, H. (1999). Sulfate is both a substrate and an activator of the voltage-dependent anion channel of Arabidopsis hypocotyl cells. Plant Physiol. *121*, 253–262.
22. Sukharev, S. (2002). Purification of the small mechanosensitive channel of Escherichia coli (MscS): The subunit structure, conduction, and gating characteristics in liposomes. Biophys. J. *83*, 290–298.
23. Xicluna, J., Lacombe, B., Dreyer, I., Alcon, C., Jeanguenin, L., Sentenac, H., Thibaud, J.B., and Cherel, I. (2007). Increased functional diversity of plant K+ channels by preferential heteromerization of the shaker-like subunits AKT2 and KAT2. J. Biol. Chem. *282*, 486–494.
24. Schaefer, M. (2005). Homo- and heteromeric assembly of TRP channel subunits. Pflugers Arch. *451*, 35–42.
25. Berrier, C., Besnard, M., Ajouz, B., Coulombe, A., and Ghazi, A. (1996). Multiple mechanosensitive ion channels from Escherichia coli, activated at different thresholds of applied pressure. J. Membr. Biol. *151*, 175–187.
26. Sukharev, S.I., Martinac, B., Arshavsky, V.Y., and Kung, C. (1993). Two types of mechanosensitive channels in the Escherichia coli cell envelope: Solubilization and functional reconstitution. Biophys. J. *65*, 177–183.